CVI
Journals.ASM.org

Macaque Paneth Cells Express Lymphoid Chemokine CXCL13 and Other Antimicrobial Peptides Not Previously Described as Expressed in Intestinal Crypts

Carissa M. Lucero,[a] Beth Fallert Junecko,[a] Cynthia R. Klamar,[a] Lauren A. Sciullo,[a] Stella J. Berendam,[a] Anthony R. Cillo,[b] Shulin Qin,[a] Yongjun Sui,[c] Sonali Sanghavi,[d] Michael A. Murphey-Corb,[b] Todd A. Reinhart[a]

Department of Infectious Diseases and Microbiology, Graduate School of Public Health, University of Pittsburgh, Pittsburgh, Pennsylvania, USA[a]; Department of Microbiology and Molecular Genetics, University of Pittsburgh School of Medicine, Pittsburgh, Pennsylvania, USA[b]; National Cancer Institute, Bethesda, Maryland, USA[c]; King Edward Memorial Hospital and Research Center, Rasta Peth, Pune, India[d]

CXCL13 is a constitutively expressed chemokine that controls migration of immune cells to lymphoid follicles. Previously, we found CXCL13 mRNA levels increased in rhesus macaque spleen tissues during AIDS. This led us to examine the levels and locations of CXCL13 by detailed *in situ* methods in cynomolgus macaque lymphoid and intestinal tissues. Our results revealed that there were distinct localization patterns of CXCL13 mRNA compared to protein in germinal centers. These patterns shifted during the course of simian immunodeficiency virus (SIV) infection, with increased mRNA expression within and around follicles during AIDS compared to uninfected or acutely infected animals. Unexpectedly, CXCL13 expression was also found in abundance in Paneth cells in crypts throughout the small intestine. Therefore, we expanded our analyses to include chemokines and antimicrobial peptides (AMPs) not previously demonstrated to be expressed by Paneth cells in intestinal tissues. We examined the expression patterns of multiple chemokines, including CCL25, as well as α-defensin 6 (DEFA6), β-defensin 2 (BDEF2), rhesus θ-defensin 1 (RTD-1), and Reg3γ *in situ* in intestinal tissues. Of the 10 chemokines examined, CXCL13 was unique in its expression by Paneth cells. BDEF2, RTD-1, and Reg3γ were also expressed by Paneth cells. BDEF2 and RTD-1 previously have not been shown to be expressed by Paneth cells. These findings expand our understanding of mucosal immunology, innate antimicrobial defenses, homeostatic chemokine function, and host protective mechanisms against microbial translocation.

Chemokines are small, chemoattractant cytokines that control the migration of cells under homeostatic and inflammatory conditions. Inflammatory chemokines are inducible during immune responses, injury, and vaccination, whereas homeostatic chemokines direct the constitutive migration of primarily immune cells to lymphoid and other tissues. CXCL13 is a member of the CXC homeostatic functional group of chemokines and functions through its receptor, CXCR5. CXCL13 was originally called B-lymphocyte chemoattractant (BLC) and was localized to the germinal centers (GCs) of lymphoid follicles in lymph nodes (LNs), spleen, and Peyer's patches (1, 2). It is detected on high endothelial venules of secondary lymphoid organs (3) and is secreted by stromal cells located in the follicles of lymphoid tissues. CXCL13 directs trafficking of B cells, follicular B helper T cells (T_{fh} cells), and subsets of dendritic cells (DCs) to lymphoid follicles. In addition to its homeostatic role in LNs and spleen, Carlsen et al. (4) noted the expression of CXCL13 in normal and diseased colonic tissues, demonstrating CXCL13 localization in aberrant lymphoid aggregates in the colonic tissue of patients with ulcerative colitis. It was suggested that CXCL13 plays a role in the formation of the gut-associated lymphoid tissues (GALT) and in the formation of irregular lymphoid aggregates of the diseased gut.

CXCL13 also has other properties. In 2003, Yang et al. (5) found that CXCL13 was among a group of chemokines with antimicrobial activity. In a standard colony-forming antimicrobial assay, CXCL13 showed antimicrobial activity against *Staphylococcus aureus* and *Escherichia coli* with 50% and 83% killing activity, respectively. Other chemokines were also found to have antimicrobial activity, indicating that chemokines can act similarly to innate host antimicrobial peptides (AMPs) that can kill and/or inactivate bacteria. The more canonical AMPs, defensins, are cationic peptides secreted by, for example, polymorphonuclear leukocytes in response to bacterial, fungal, and viral pathogens (6). The functions of defensins overlap the functions of chemokines as subsets of both can be chemotactic for CD4 and CD8 cells and DCs, and they both can stimulate degranulation of leukocytes (7). In addition, the structures of chemokines and defensins are similar in that they both contain a region with highly conserved cysteine residues. Furthermore, some AMPs possess antiviral properties, including against HIV-1. Wang et al. (8) measured the capabilities of α- and θ-defensins to bind to HIV-1 and found that retrocyclin-2 binds to gp120 and CD4 and inhibits HIV-1 infection (8). Human α-defensins 1, 2, and 3 are produced by immature DCs, bind to gp120, and potentially protect against disease progression (9).

Previously, we found that during simian immunodeficiency virus (SIV) infection of macaques, CXCL13 mRNA expression was upregulated in lymphoid tissues (10). To investigate additional roles for CXCL13 in the host response to SIV infection, we have examined the levels and patterns of expression of CXCL13 in macaque lymphoid and intestinal tissues by *in situ* hybridization

Received 30 October 2012 Returned for modification 11 December 2012
Accepted 12 June 2013
Published ahead of print 26 June 2013
Address correspondence to Todd A. Reinhart, reinhar@pitt.edu.

doi:10.1128/CVI.00651-12

(ISH) and immunohistochemistry (IHC). We found that CXCL13 expression was altered during pathogenic SIV infection in lymphoid tissues. In addition, we discovered that CXCL13 was also expressed by Paneth cells, which are an epithelial cell subset localized to intestinal crypts and specialized for AMP production. Analyses of other chemokines and AMPs revealed that CXCL13 was uniquely expressed by Paneth cells and revealed that other known AMPs are also expressed specifically by Paneth cells. These findings suggest multiple roles for CXCL13 in host immunobiology, including as a tool for protection of intestinal epithelial stem cells and possibly for helping to shape the intestinal microbiome.

MATERIALS AND METHODS

Animals and tissues. These studies were performed under the approval and guidance of the University of Pittsburgh Institutional Animal Care and Use Committee. Adult cynomolgus macaques (*Macaca fascicularis*) were used in this study and were inoculated intrarectally with the pathogenic SIV/DeltaB670 isolate (11). These animals and their clinicovirologic states have been described previously (12–14). Fixation and processing of tissues at necropsy were completed as described previously (15). Tissues used for visualization of Paneth cells were postfixed in 4% paraformaldehyde and then dehydrated in graded ethanols. These tissues were then stained by Lendrum's procedure modified by extending tartrazine staining for a period of 5 h and 45 min.

Cloning of macaque DEFA6, BDEF2, and RTD-1 cDNAs. To generate α-defensin 6 (DEFA6), β-defensin 2 (BDEF2), and rhesus θ-defensin 1 (RTD-1) cDNAs, RNA was purified from cryopreserved cynomolgous ileal tissue, and cDNA synthesis was performed as described previously (16). Human Reg3γ cDNA was purchased from Open Biosystems (ThermoFisher Scientific, Lafayette, CO). The primers used for PCR amplification were designed based on the corresponding human sequences for α-defensin 5 and β-defensin 2 (GenBank accession no. AY859407 and AF040153, respectively). The resultant forward and reverse primers were rhDEFA5_F2_CF (5′-CTCACCATCCTTGCTGCCATTC-3′) and rhDEFA5_R2_CF (5′-CTAGGAAGCTCGGCGACAGCA-3′) for DEFA6, SS_HBD2_F1 (5′-CATCAGCCATGAGGGTCTTG-3′) and SS_HBD2_R1 (5′-CTCATGGCTTTTTGCAGCATT-3′) for BDEF2, and SS_RTD1_F1 (5′-GGAGACCCGGGACAGAGGAC-3′) and SS_RTD1_R1 (5′-AAAGAGAGAAATCTTGCAACAAGGTA-3′) for RTD-1. PCR products were ligated into the pGEM-T vector (Promega), and the DNAs were sequenced.

***In situ* hybridization and immunohistochemistry.** *In situ* hybridization (ISH) for rhesus CXCL13, CCL25, α-defensin 6 (DEFA6), β-defensin 2 (BDEF2), RTD-1, and Reg3γ mRNAs was performed as described previously (15, 17). Immunohistochemistry (IHC) for CXCL13 protein was performed on tissues as previously described (18). CXCL13 protein was detected by heating tissues in the microwave in Dako target retrieval buffer (Dako, Carpenteria, CA) and then incubating them with a goat anti-CXCL13 polyclonal antibody (1:50) (R&D Systems; catalog no. AF801) for 1 h. A parallel tissue on the same slide was incubated with a goat IgG antibody (1:500) (Dako, catalog no. AB108C). The primary antibodies were then detected with an anti-goat SuperPicture kit (Zymed Laboratories, South San Francisco, CA), according to the manufacturer's instructions. All tissues were subsequently counterstained with hematoxylin (Fisher Chemicals, Fairlawn, NJ).

Simultaneous detection of CXCL13 protein and either DEFA6, BDEF2, DEFA1, RTD-1, or Reg3γ mRNAs was performed by conducting the previously described IHC procedure prior to completion of the ISH protocol. Briefly, tissues were pretreated in Dako target retrieval buffer, rinsed, and then incubated with goat anti-CXCL13 primary antibody for 1 h at room temperature. Tissues were then rinsed and incubated with anti-goat secondary antibody conjugated to peroxidase (SuperPicture kit; Invitrogen). Sections were rinsed and incubated with the substrate diaminobenzidine (DAB) for 10 min. Upon completion, slides were rinsed briefly in water and then immediately placed in 0.1 M triethanolamine with 500 μl acetic anyhydride to acetylate the tissue sections to reduce nonspecific riboprobe binding. The remaining ISH steps were followed as previously described.

Immunofluorescence and image capture. Two-color immunofluorescence detection of CXCL13 and DEFA6 was performed by incubating tissues simultaneously with anti-CXCL13 conjugated to donkey anti-goat Alexa Fluor 647 and anti-DEFA6 (1:1,000) (Sigma, catalog no. HPA019462) conjugated to donkey anti-rabbit Alexa Fluor 488. All tissue sections for immunofluorescence were treated with Autofluorescence Eliminator (Chemicon International) before being mounted with Prolong Gold antifade with DAPI (4′,6-diamidino-2-phenylindole) for nuclear staining (Molecular Probes). Images of immunohistochemistry and immunofluorescence tissue sections were captured on a Nikon (Melville, NY) E600 microscope mounted with a SPOT charged-coupled device (CCD) camera (Diagnostic Instruments, Sterling Heights, MD). The MetaVue software package (Universal Imaging, West Chester, PA) was used to view captured images. Confocal microscopy images were captured on an Olympus Fluoview 500 microscope.

DLR assays. The HEK293T cell line was used for CXCL13 promoter activity analyses using a dual-luciferase reporter (DLR) assay (Promega). Cells (8×10^5) were plated in poly-L-lysine-coated 6-well culture plates (Corning) 24 h prior to transfection using PolyJet (SignaGen) per the manufacturer's recommendations with 1 μg of total plasmid DNA per well. Cell lysates were harvested after in-well lysis with Promega passive lysis buffer (0.5 ml), frozen and thawed three times, and cleared by microcentrifugation at 4°C. The DLR assays were performed in white polystyrene 96-well plates (Costar) with 20 μl of lysate per well and read using a FLUOstar Optima with luminescence readings (firefly luciferase and then *Renilla* luciferase) taken from above individual wells. Cotransfection with plasmid pGL4.74 (Promega) encoding *Renilla* luciferase allowed normalization for transfection efficiency differences. Following normalization of firefly luciferase values to *Renilla* luciferase values, the ratios were multiplied by a constant of 10,000. The positive-control plasmid, pGL2-Control (Promega), was included in all transfection experiments, as was the promoterless pGL2-Basic vector (Promega). Data analyses were performed using MARS analysis software (BMG Labtech), with further analyses using Prism software (GraphPad). Short-chain fatty acid (SCFA) stimulations with sodium butyrate, sodium acetate, sodium propionate, or sodium lactate (Sigma) were performed at 5 mM 24 h before harvesting of cell lysates. Trichostatin A and 5-azacytidine (Sigma; 5 μM) pretreatments were performed for 24 h prior to sodium butyrate stimulation.

RESULTS

CXCL13 mRNA and protein are differentially localized in macaque lymphoid tissues. To examine CXCL13 expression in lymphoid tissues and to define potential changes in CXCL13 expression during pathogenic SIV infection, we examined mRNA expression patterns in lymph node (LN) and spleen tissues of cynomolgus macaques by ISH. The tissues examined were collected at necropsy from cynomolgus macaques that were either uninfected or were infected intrarectally with the SIV/DeltaB670 pathogenic strain (11) and sacrificed during acute infection (2 weeks postinfection [p.i.]) or upon development of AIDS (14 to 62 weeks p.i.), which was defined by weight loss, loss of $CD4^+$ T lymphocytes, and/or development of opportunistic infections, such as *Pneumocystis jirovecii* pneumonia. These animals and their clinicovirologic states have been presented previously (12–14).

Cells producing CXCL13 mRNA localized to a ring around germinal centers (GCs) in LN tissue sections (Fig. 1A). Subjacent tissue sections were immunostained for CXCL13 protein, and, unexpectedly, CXCL13 protein signal was intensely localized to the center of the GCs (Fig. 1A). In these regions, there were networks of CXCL13 clearly visible after IHC and immunofluorescent staining for CXCL13 in LN (Fig. 1A). In LN paracortices,

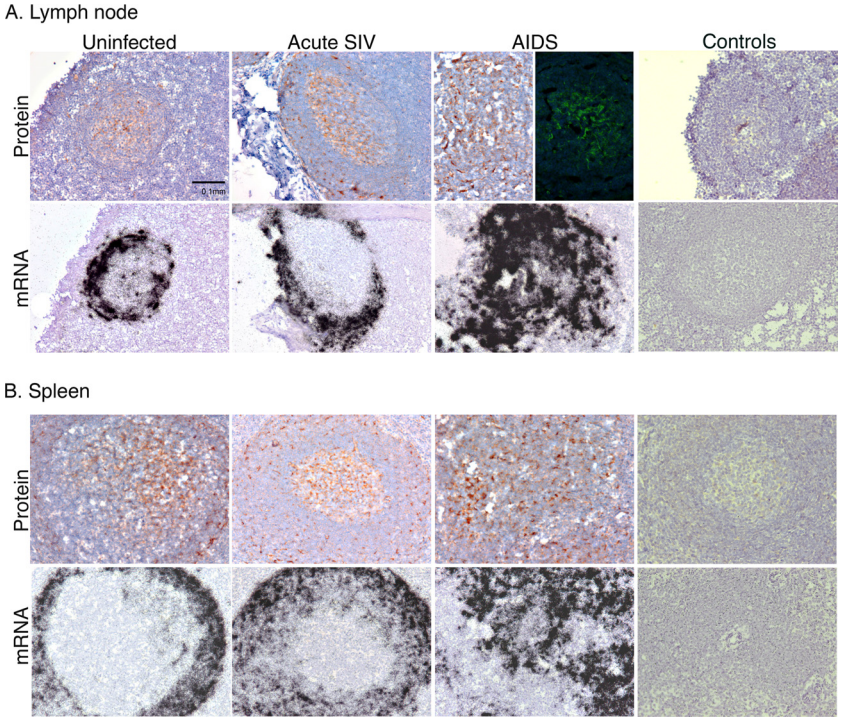

FIG 1 Localization of CXCL13 mRNA and protein in macaque lymph node and spleen. CXCL13 protein was detected by IHC (brown signal) or immunofluorescent staining (LN, AIDS, top row) in lymph node (A) or spleen (B) at the indicated SIV-related disease state. Parallel controls performed with control antibody or cognate sense riboprobes are presented to the far right. Original magnifications, ×200.

there also were individual cells that stained for CXCL13. Parallel staining of subjacent tissue sections with control goat Ig did not yield specific signal (Fig. 1A, right). The mRNA and protein expression patterns of CXCL13 in macaque spleen tissues were similar to those in LNs (Fig. 1B). These data indicate that CXCL13 producer cells are localized in a microanatomic compartment distinct from and immediately adjacent to that harboring the highest levels of CXCL13 protein in the centers of GCs.

CXCL13 expression in LN and spleen tissues was also examined across SIV disease states by staining tissues from SIV/DeltaB670-infected animals that had been previously examined for inflammatory chemokine expression in lymphoid (14) and lung (13) tissues. We compared expression patterns in LNs from uninfected, acutely SIV-infected, and AIDS-developing macaques and found that CXCL13 mRNA expression was upregulated during acute infection and maintained at high levels during AIDS (Fig. 1A). In contrast, CXCL13 protein expression increased to a limited extent across disease states. Parallel analysis of spleen tissues from the same macaques yielded similar results (Fig. 1B).

CXCL13 is expressed by Paneth cells. Intestinal tissues are considered to be one of the largest lymphoid organs and are a site in which many $CD4^+$ T lymphocytes are lost during HIV-1 and SIV infection (19). Therefore, we examined the microanatomic distribution of CXCL13 in different regions along the gastrointestinal (GI) tract. Using ISH and IHC, we observed mRNA and protein expression in lymphoid follicles throughout the intestines, including in duodenum, jejunum, ileum, and colon, again with $mRNA^+$ producer cells distributed in a three-dimensional spherical shell surrounding high levels of CXCL13 protein within GCs (not shown). Interestingly, we observed intense expression of CXCL13 mRNA and protein in a subset of cells in the crypts of Lieberkühn (Fig. 2). Cells expressing CXCL13 in crypts were observed in duodenal, jejunal, and ileal tissues from all 16 macaques studied but were not observed in colon in any of these animals.

Paneth cells are specialized intestinal epithelial cells that produce AMPs and usually are found only in the small intestine (20). The regional distribution of CXCL13 expression in intestinal crypts we observed could be due to its expression by Paneth cells. To determine if Paneth cells were the source of CXCL13 in the intestinal crypts, we individually and simultaneously stained for α-defensin 6 (DEFA6), which is an AMP uniquely expressed by Paneth cells. In macaque small intestine, we found Paneth cell secretory granules (Fig. 3A), DEFA6 protein (Fig. 3B), and DEFA6 mRNA (Fig. 4A) localized to intestinal crypts in patterns identical to those obtained for CXCL13. Similar to CXCL13, DEFA6 was expressed in jejunum and ileum, but not in colon. Simultaneous IHC for CXCL13 protein and ISH for DEFA6 mRNA demonstrated colocalization to the same cells in crypts (Fig. 3C). In addition, two-color immunofluorescence staining and confocal microscopy confirmed that CXCL13 and DEFA6 are coexpressed by Paneth cells in intracellular granules, with most CXCL13 signal overlapping a large proportion of the DEFA6 signal (Fig. 3H). These findings confirm that that source of CXCL13 in intestinal crypts is the Paneth cell and are to our knowledge the first to show the expression of a lymphoid homeostatic chemokine by this specialized intestinal epithelial cell.

CXCL13 is uniquely expressed by Paneth cells among a subset of CC and CXC chemokines. To determine whether other chemokines also were expressed strongly in intestinal crypts, we examined the localization of mRNA producer cells of multiple

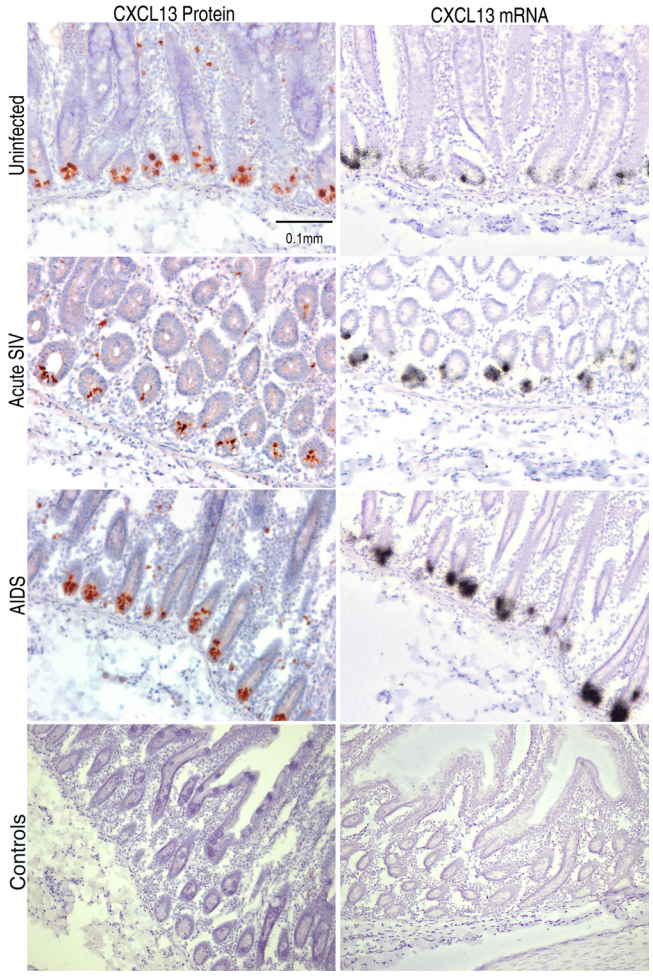

FIG 2 Expression of CXCL13 mRNA and protein in intestinal crypts. IHC (brown signals) and ISH (black silver grain signals) were performed on macaque jejunum, revealing localization of CXCL13 producer cells in the intestinal crypts of Lieberkühn. Parallel controls performed with control antibody or sense riboprobes are shown in the bottom two images. Original magnifications, ×200.

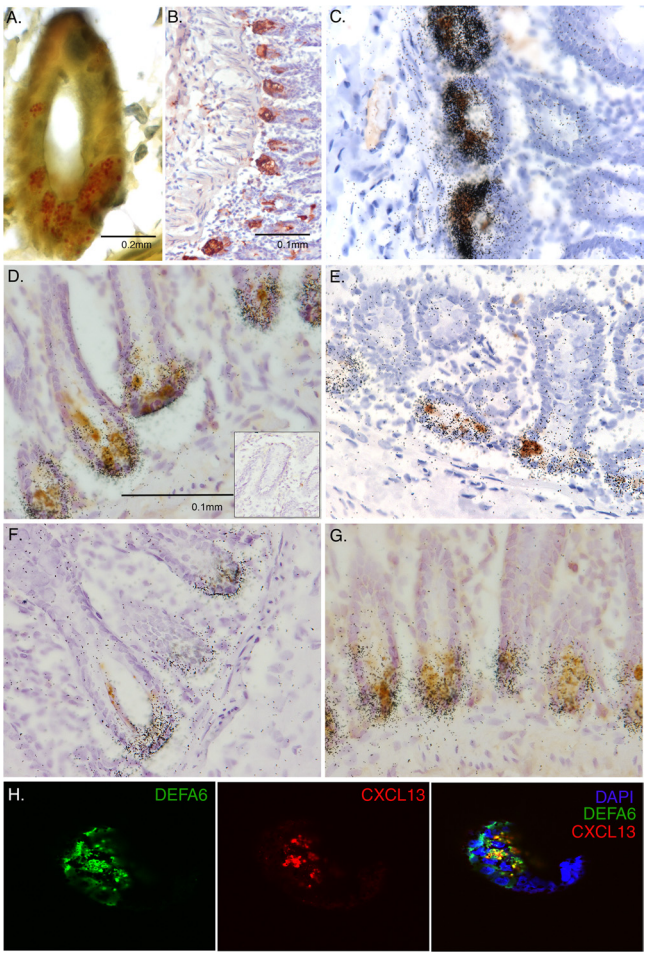

FIG 3 Identification of Paneth cells as producers of CXCL13 and other antimicrobial peptides. (A) Phloxine-tartrazine staining was performed for Paneth cell granules in the crypts of Leiberkühn in macaque ileum. (B) IHC was performed to detect DEFA6, a marker for Paneth cells, in macaque ileum. The brown signal indicates the location of the bound antibodies. (C) ISH for DEFA6 mRNA (black silver grains) was combined with IHC for CXCL13 (brown signal) in macaque ileum. IHC for CXCL13 protein was combined with ISH for mRNAs encoding (D) DEFA1, (E) BDEF2, (F) RTD-1, or (G) Reg3γ in macaque ileum. The inset in panel D is a representative image following ISH with the corresponding sense control probe and IHC with an isotype control antibody. (H) Immunofluorescence staining and confocal microscopic detection of DEFA6 and CXCL13 was performed on macaque ileum.

chemokines along the macaque GI tract. These included CCL25, a ligand for CCR9 that directs the trafficking of intestinal homing T and B lymphocytes (Fig. 4D to F), as well as CXCL1, CXCL9, CXCL10, CXCL11, CXCL12, CCL19, CCL20, and CCL21. CCL25 is known to be expressed by small intestinal epithelium, and consistent with this, the mRNA expression patterns for CCL25 differed greatly from those for CXCL13, with CCL25 producer cells found uniformly across the epithelium of the small intestine and not in the GALT, Paneth cell-laden crypts, or colon. Cells producing the other chemokines examined were not localized to intestinal crypts and therefore were not in Paneth cells (not shown).

Expression of other AMPs by Paneth cells. Given the clear expression of CXCL13 by Paneth cells, suggesting it has antimicrobial functions in the intestine, we next examined whether other AMPs not previously recognized as expressed by Paneth cells are also produced by them. Although both DEFA5 and DEFA6 are AMPs produced by Paneth cells, β-defensins have not been localized to these specialized cells. Unexpectedly, β-defensin 2 (BDEF2) mRNA-producing cells also were localized to intestinal crypts (Fig. 4G), and simultaneous ISH for BDEF2 mRNA and IHC for CXCL13 protein revealed colocalization to the same cells in crypts (Fig. 3E). Similarly, rhesus θ-defensin 1 (RTD-1) was expressed specifically in intestinal crypts (Fig. 4H) and Paneth cells (Fig. 3F). Macaques are not known to express the AMP Reg3γ as an AMP in Paneth cells (21, 22). By using ISH, we confirmed that Reg3γ was expressed in crypts throughout the small intestine in cynomolgus macaques but was absent from the colon (Fig. 4I). In summary, these findings provide the first evidence that in macaques BDEF2 and RTD-1 are expressed by Paneth cells and expand our understanding of the repertoire of AMPs used by these cells to protect the crypts and shape the intestinal milieu.

To determine whether SIV infection impacted levels of expression of Paneth cell AMPs, including CXCL13, we examined tissues from animals in different stages of SIV infection. Admittedly these

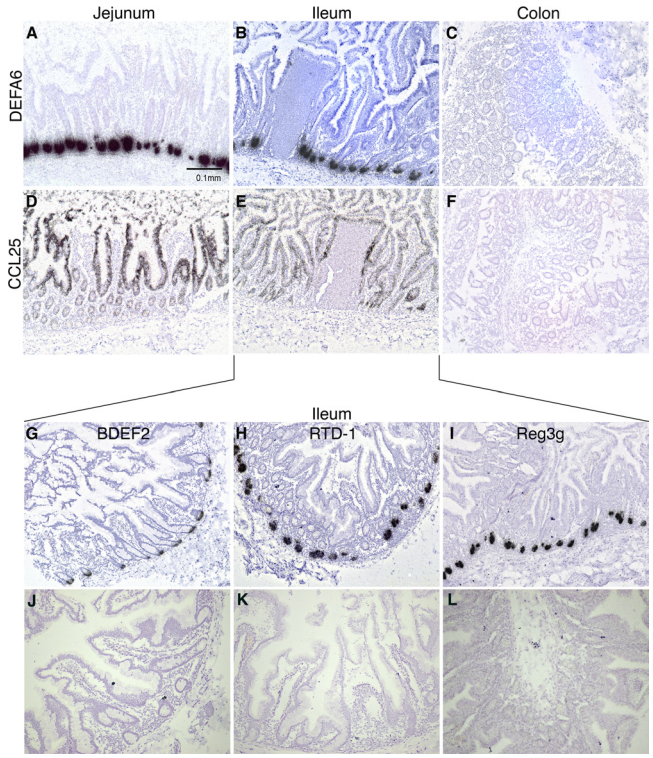

FIG 4 Localization of antimicrobial peptide and CCL25 mRNAs in intestinal tissues. *In situ* hybridizations were performed to localize DEFA6 (A to C) and CCL25 (D to F) mRNAs in uninfected, acutely infected, and AIDS-developing macaque jejunum, ileum, and colon tissue sections. ISHs were also performed to detect BDEF2 (G), RTD-1 (H), and Reg3γ (Reg3g) (I) mRNAs in uninfected macaque jejunum. ISH results obtained with parallel hybridization with the cognate sense control riboprobes are shown in panels J to L. Original magnifications, ×100.

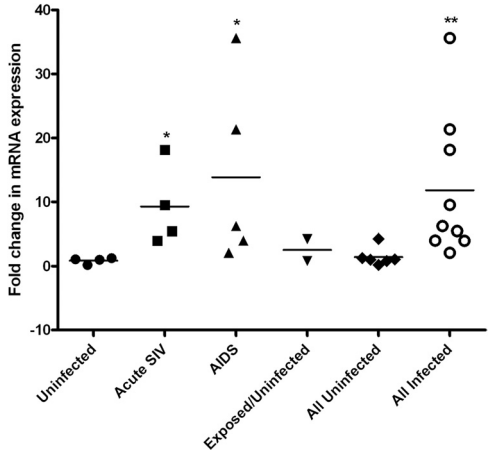

FIG 5 Measurement of DEFA6 mRNA levels in macaque ileum. Real-time RT-PCR (TaqMan) was used to measure DEFA6 mRNA levels in homogenized ileum, which was normalized to the endogenous control β-GUS, and then all values were calibrated to one uninfected sample. Shown are the individual values and the means for each group. Statistically significant differences were observed relative to the uninfected group (Mann-Whitney test): *, $P < 0.05$; **, $P < 0.01$.

intestinal tissues were fixed and cryopreserved without attention at the time to tissue orientation and interest in Paneth cells, so we were not able to reliably ensure a uniform representation of crypts and Paneth cells for quantitative analysis of tissue sections. However, at a qualitative level, differences in the intensities of the IHC signals for CXCL13 and DEFA6 did not appear to change, and the ISH signals appeared to increase slightly during AIDS. Multiple attempts to use a commercially available real-time reverse transcription (RT)-PCR assay for macaque *cxcl13* mRNA or to develop an assay in house failed to meet quality control requirements, and therefore accurate measurement of *cxcl13* mRNA in lymphoid and intestinal tissue RNA preparations was not achieved. In contrast, the real-time RT-PCR assay for DEFA6 was robust (not shown), and DEFA6 is known to be expressed uniquely by Paneth cells (e.g., Fig. 4A). Using this assay, we found that the levels of expression for this AMP increased ~10-fold during acute infection and AIDS in the ileum (Fig. 5). These changes were positively correlated with SIV plasma virus loads (PVLs) ($\log_{10}$ SIV PVLs versus ileum DEFA6 mRNA levels, $r^2 = 0.53$, $P = 0.04$). This increase in defensin expression is consistent with a recent report that SIV infection leads to induction of rhesus enteric defensin (RED) (19). We also developed real-time RT-PCR assays (SYBR green) for RTD-1 and BDEF2. The RTD-1 assay was not of sufficient robustness to allow quantitation, but the BDEF2 assay was robust. BDEF2 mRNA levels in homogenized macaque ileum did not change early or late after SIV infection (data not shown). Altogether, these data revealed that SIV infection impacts the expression of DEFA6 by Paneth cells.

The *cxcl13* promoter is stimulated by the short-chain fatty acid sodium butyrate. To understand better the regulation of CXCL13 expression and its strong expression by Paneth cells, we cloned, sequenced, and functionally examined the cynomolgus (cyCXCL13p) and rhesus (rhCXCL13p) macaque *cxcl13* promoters. rhCXCL13p and cyCXCL13p were 99% homologous to one another, and each was 94% homologous to the corresponding human sequences. Basal and cytokine-induced responses of the macaque *cxcl13* promoters were measured by transient transfection of HEK293T cells with a reporter plasmid containing the *cxcl13* promoter driving luciferase as a readout. Our results showed that neither of the proinflammatory cytokines tumor necrosis factor alpha (TNF-α) nor interleukin-1β (IL-1β) led to induction of luciferase activity from the rhesus or cynomolgus *cxcl13* promoters (Table 1), although they potently increased luciferase activity from the corresponding *ccl20* promoters by up to 40-fold (data not shown; unpublished data). In contrast, we found that sodium butyrate, a short-chain fatty acid (SCFA) that is a product of bacterial metabolism and has histone deacetylase (HDAC) inhibitory activity, induced the macaque *cxcl13* promoters by about 10-fold (Table 1). Sodium butyrate treatment of cells transfected with a promoterless pGL2-Basic plasmid, showed no change in the level of firefly luciferase activity compared to that in untreated cells, indicating that this intestinal short-chain fatty acid was not acting broadly on any DNA sequence upstream of the luciferase open reading frame (ORF). Treatment of transiently transfected cells with other SCFAs revealed that sodium propionate also stimulated the *cxcl13* promoter by 2- to 3-fold, whereas sodium lactate and sodium acetate had only minimal effects (Table 1).

Sodium butyrate has histone deacetylase (HDAC) inhibitory activity (43), and to determine whether sodium butyrate's effects on the cxcl13 promoter were due to this effect, we compared its ability to modulate the *cxcl13* promoter after pretreatment of cells

TABLE 1 Cytokine and SCFA responses of the *Cxcl13* promoters from cynomolgus and rhesus macaques

Treatment group[a]	Activity (RLU) of CXCL13p type[b]:	
	Cynomolgus	Rhesus
Promoter controls[c]		
Mock	0 ± 0	0 ± 0
No promoter	287 ± 109	260 ± 128
SV40p	29,608 ± 10,280	21,935 ± 3,938
Cytokine stimulations[c]		
Untreated	1,964 ± 452	1,681 ± 502
TNF-α	1,817 ± 738	1,486 ± 356
IL-1β	1,810 ± 534	1,454 ± 510
TNF-α + IL-1β	1,732 ± 315	1,539 ± 452
IFN-γ	1,625 ± 463	1,540 ± 489
LPS	2,215 ± 236	1,307 ± 426
Sodium butyrate stimulations[c,d]		
Untreated	36,838 ± 6,155	29,537 ± 6,727
Sodium butyrate	353,262 ± 32,353	267,587 ± 50,801
SCFA stimulations[c,d]		
Mock	0 ± 0	0 ± 0
No promoter	524 ± 82	524 ± 82
SV40p	22,122 ± 2,588	22,122 ± 2,588
Untreated	5,488 ± 4,747	5,638 ± 1,483
Sodium butyrate	44,790 ± 4,985	38,205 ± 6,170
Sodium propionate	19,218 ± 2,777	9,982 ± 6,137
Sodium lactate	8,250 ± 777	5,953 ± 765
Sodium acetate	7,073 ± 2,892	4,049 ± 2,505
SCFA stimulations after pretreatment[e]		
Mock	0 ± 0	ND[f]
No promoter	0.04 ± 0.03	
SV40p	1.00 ± 0	
Untreated	0.16 ± 0.13	
Sodium butyrate	0.78 ± 0.41	
TSA pretreatment	1.66 ± 0.46	
Sodium butyrate + TSA pretreatment	1.86 ± 0.23	
5-Aza pretreatment	0.13 ± 0.14	
Sodium butyrate + 5-Aza pretreatment	0.81 ± 0.16	
TSA + 5-Aza pretreatment	1.98 ± 0.08	
Sodium butyrate TSA + 5-Aza pretreatment	2.20 ± 0.39	

[a] Abbreviations: SV40p, simian virus 40 promoter; TNF-α, tumor necrosis factor α; IL-1β, interleukin-1β; IFN-γ, gamma interferon; LPS, lipopolysaccharide; SCFA, short-chain fatty acid; TSA, trichostatin A; 5-Aza, 5-azacytidine.
[b] All data presented in this table were combined from three independent experiments, each performed in duplicate. Values are means ± SD.
[c] The values presented are relative luminescence units (RLU) in which the indicated promoter drove firefly luciferase expression, the levels of which were normalized to expression of *Renilla* luciferase driven by the herpes simplex virus (HSV) thymidine kinase (TK) promoter on a cotransfected plasmid (dual-luciferase reporter [DLR] assay, as described in Materials and Methods).
[d] The values from the sodium butyrate stimulations are the firefly luciferase activity not normalized to *Renilla* luciferase activity because sodium butyrate also stimulated the HSV-TK promoter of the pGL4.74 vector, abrogating its utility for transfection normalization. The SCFA stimulations with different SCFAs were performed independently and subsequently to the sodium butyrate-only studies.
[e] The firefly luciferase values (not normalized to *Renilla* luciferase) were all normalized to the positive control (simian virus 40 promoter [SV40p]).
[f] ND, not determined.

with pharmacologic modulators of chromatin compaction. Pretreatment of cells with trichostatin A, a broad-spectrum inhibitor of HDACs, increased luciferase activity driven by the *cxcl13* promoter by almost 2-fold, with no additional increase observed when cells were treated with sodium butyrate after trichostatin A pretreatment (Table 1, bottom). In contrast, pretreatment of cells with the DNA methyltransferase inhibitor 5-azacytidine did not stimulate the *cxcl13* promoter and did not inhibit the ability of sodium butyrate to do so. Altogether, these findings suggest that pro-inflammatory cytokines are not likely to control the expression of CXCL13 by Paneth cells or stromal cells, whereas the bacterially produced SCFA sodium butyrate could contribute to CXCL13 expression by Paneth cells primarily through its HDAC inhibitory activity.

DISCUSSION

CXCL13 is a homeostatic chemokine that controls, in large part, the migration of B cells, follicular helper T (T_{fh}) cells, and DCs into the follicles of secondary lymphoid tissues. Because CXCL13

is responsible for trafficking of B cells and T_{fh} cells into the marginal zones of follicles, it is possible that modifications to its expression might contribute to the B cell dysfunction occurring in HIV-1 infection. Here we have examined the expression patterns of CXCL13 in lymphoid tissues, including intestine, and found that SIV infection causes a more disordered distribution of CXCL13 producer cells in LN and spleen and that CXCL13 is expressed by Paneth cells in the small intestine.

A limited number of studies have examined CXCL13 in the context of HIV-1 or SIV infection. CXCL13 levels are elevated in plasma during HIV-1 infection and correlate with levels of CXCL10 in advanced disease (23). In addition, CXCL13 production by B cells is increased in HIV-1-infected patients and there is increased migration toward CXCL13 by peripheral blood B cells from patients with advanced disease (24). CXCL13 protein expression during HIV-1-driven follicular hyperplasia is associated with the GC light zone and the follicular DC (FDC) network. These reports are consistent with our findings of an expansion and redistribution of CXCL13 producer cells in LNs and spleen.

During pathogenic SIV infection, we had previously identified CXCL13 as one of two chemokines with increases in mRNA expression in spleen tissues (10). We focused here on obtaining an improved understanding of the immunobiology of this chemokine in a robust macaque model for HIV/AIDS. We found CXCL13 protein was centrally located within GCs, whereas CXCL13 mRNA was generally localized in cells defining a shell in the mantle and marginal zones of follicles. This disparate microanatomic localization of CXCL13 mRNA and protein was unexpected and underscores the complexity of the *in vivo* immunobiology of chemokines within tissues. The mechanism by which CXCL13 is concentrated within GCs, compared to the spherical shell of producer cells and the adjacent paracortices, is not clear. There are a number of possible mechanisms, however. For example, the intense staining in the center of the sphere circumscribed by the CXCL13 producer cells could be a consequence of bidirectional diffusion away from the producer cells in both the central follicular and paracortical directions, resulting in an increased overall concentration within GCs and a reduced concentration in paracortices. Alternatively, CXCL13 release might be polarized and limited to the follicular surfaces of producer cells. This would lead to lower concentrations of CXCL13 outside the GCs and increased concentrations within the GCs. In addition, there might be an active transport mechanism that maintains the extracellular CXCL13 within the GC, perhaps piggybacking on cells migrating toward the GC or in microchannels. The latter would be consistent with the thin, cord-like structures we have observed (e.g., Fig. 1) in LNs and spleen. Furthermore, there might be differential expression of proteases that process CXCL13 in lymphoid tissue microcompartments, with a higher concentration of proteases in the surrounding paracortices relative to the inside the GCs. Such compartmentalization of proteases would be consistent with the ability of GCs to harbor immune complexes on FDC surfaces for long periods of time (25–27), and it is possible that FDCs also serve a depot function for CXCL13 as well. Regardless of the mechanism(s), the compartmentalization of CXCL13 within lymphoid tissue GCs is consistent with its role in bringing T_{fh} cells, B cells, and DCs together.

In this study, we found there were also disease-specific changes in CXCL13 expression in lymphoid tissues, with the $mRNA^+$ producer cells expanding more broadly into the GCs and surrounding microcompartment as the course of infection progressed. Recently, increases in LN T_{fh} cells in HIV-1 infected individuals were observed despite the overall reduction in the number of $CD4^+$ T cells that occurs during infection (28). Given that T_{fh} cells express CXCR5, the CXCL13 receptor, as well as CXCL13 *per se*, the more distributed pattern of CXCL13 producer cells we observed could be driven by recruitment and/or expansion of T_{fh} cells. In addition, a recent comparison between uninfected and SIV-infected rhesus macaque T_{fh} cells revealed a 5-fold induction of CXCL13 expression in T_{fh} cells that were SIV infected (29). B cell affinity maturation and isotype switching occur in GCs (30), and given the known B cell dysfunction that occurs during HIV-1 and SIV infection (31–34), it is conceivable that a chemokine that orchestrates the migration of these cells into follicles could contribute to humoral immune response abnormalities that arise during infection. Consistent with this notion, it has been argued recently that there is a decrease in memory B cell levels due to the distortion of the B cell population toward GC B cells and plasma cells during chronic HIV-1 infection (28).

A major finding from the studies presented here was the discovery that CXCL13 was expressed by Paneth cells. Paneth cells are specialized intestinal epithelial cells that express AMPs and proinflammatory cytokines that contribute to innate immunity (20). The AMPs secreted by Paneth cells have several overlapping roles in the intestine (35), including shaping the composition of and limiting the number of commensals populating the small intestine, protecting the intestine and its stem cells from invading pathogens, and acting as paracrine signaling molecules (35). It has been argued that Paneth cells are responsible for the homeostatic environments surrounding the intestinal villi and crypts by regulating microbe infiltration (36). Given the expression of CXCL13 by Paneth cells, one of its major functions in the small intestine is likely as an AMP, which would not have been anticipated for an LN homeostatic chemokine. The same regional distribution of CXCL13 along the GI tract as other Paneth cell-expressed AMPs and the colocalization of CXCL13 and DEFA6 in Paneth cells support the interpretation that CXCL13 likely functions *in vivo* as an AMP. Furthermore, many chemokines have antimicrobial activity in *in vitro* assays, including CXCL13 (5). Among the microbes against which CXCL13 exhibited antimicrobial activity were the intestinal bacteria *E. coli* and *S. aureus* (5). Therefore, we posit that our findings here provide the strongest *in vivo* evidence, albeit indirect, that chemokines can function as AMPs. It was surprising, however, that the chemokine discovered as expressed by the AMP-producing Paneth cell was a chemokine previously relegated to that of a lymphoid tissue homeostatic chemokine.

In addition to CXCL13, we show here that BDEF2, RTD-1, and Reg3γ are also expressed by macaque Paneth cells, this report being the first to demonstrate this for BDEF2 and RTD-1. β-Defensins are expressed by epithelial cells in multiple mucosal tissues, including skin, stomach, and colon. However, they have not been reported as expressed by Paneth cells. Interestingly, in addition to AMP activity, β-defensins also possess chemotactic activity. For example, BDEF2 is chemotactic for $CCR6^+$ cells (37), which as a regulator of Th17 migration (38) could participate in IL-17's contributions to intestinal epithelial integrity. The θ-defensins are cyclic defensins originally isolated from leukocytes and bone marrow of rhesus macaques (39). Rhesus θ-defensins and repaired human retrocyclin have broad antimicrobial properties with inhibitory effects on HIV-1, influenza virus, and multiple

bacterial species. As with BDEF2, predominant expression in the GI tract by Paneth cells has not been reported. Finally, Reg3γ is an AMP expressed by murine Paneth cells (21), and our findings reveal the same for macaque Reg3γ. Of these AMPs, we were able to show that DEFA6 was increased following SIV infection and these changes were positively correlated with plasma viral loads. Comparison of the sequence of our DEFA6 cDNA and that of RED6 revealed they are the same gene, and therefore our finding of increased DEFA6 by Paneth cells in cynomolgus macaques is consistent with findings by Zaragoza et al. (19) in rhesus macaques. It is not clear the mechanism(s) by which SIV infection leads to DEFA6 upregulation, whereas, for example, BDEF2 is not upregulated. Nonetheless, increased AMP expression could have effects on the intestinal microbiome or could affect the levels of local inflammation. Since both of these effects could impact intestinal epithelial barrier integrity, extrapolating to HIV-1-infected individuals, outcomes might include increased microbial translocation and systemic immune activation (40). Altogether, these findings increase our understanding of the composition of the AMP repertoire produced by Paneth cells, the diversity of which likely reflects the diverse set of microbes targeted as an innate protective mechanism against microbial translocation in the intestinal crypts.

Little is known about the *cxcl13* transcriptional promoter, and the limited expression of CXCL13 predominantly by GC-associated cells in lymphoid follicles and by Paneth cells indicates the *cxcl13* promoter is tightly regulated. In our hands, even the potent inflammatory cytokines TNF-α and IL-1β failed to stimulate expression from the rhesus or cynomolgus macaque *cxcl13* promoter, although *ccl20* promoter constructs were strongly induced by the same cytokines (not shown; unpublished data), indicating that HEK293T cells possess the corresponding, functionally active receptors. SCFAs, such as sodium butyrate, are produced by intestinal bacteria (41, 42), and we found that the macaque *cxcl13* promoter was induced by this product of bacterial fermentation, most likely due to its HDAC inhibitory activity (43–45), since it did not stimulate the *cxcl13* promoter above what was achieved with the broad-spectrum HDAC inhibitor trichostatin A (Table 1). The antimicrobial cathelicidin LL37 is also stimulated by sodium butyrate (43, 44, 46, 47). The upregulation of the *cxcl13* promoter by microbial products, similar to LL37, is consistent with our interpretation that CXCL13 has AMP function in the intestine.

Overall, the findings presented here support the notion that chemokines function as AMPs. This has been demonstrated for many chemokines *in vitro*, but localization of CXCL13 to Paneth cells, which are specialized for production of AMPs, and transcriptional induction of the *cxcl13* promoter by the intestinal bacterial product sodium butyrate provide strong support that at least a subset of chemokines provide antimicrobial function *in vivo*. That a lymphoid homeostatic chemokine is functioning in these dual capacities is intriguing, and it will be interesting to unravel the structural and biochemical aspects of these different functions of CXCL13.

ACKNOWLEDGMENTS

This project was supported by NIH grants AI060422 (T.A.R.) and AI90825 (M.M.C.), the K. Leroy Irvis Scholarship program at the University of Pittsburgh (C.M.L.), and NIH T32 AI065380 (Pitt AIDS Research Training Program) from the NIAID.

We thank Velpandi Ayyavoo and Tianyi Wang for helpful discussions and advice regarding the luciferase assays.

REFERENCES

1. **Legler DF, Loetscher M, Roos RS, Clark-Lewis I, Baggiolini M, Moser B.** 1998. B cell-attracting chemokine 1, a human CXC chemokine expressed in lymphoid tissues, selectively attracts B lymphocytes via BLR1/CXCR5. J. Exp. Med. **187:**655–660.
2. **Gunn MD, Ngo VN, Ansel KM, Ekland EH, Cyster JG, Williams LT.** 1998. A B-cell-homing chemokine made in lymphoid follicles activates Burkitt's lymphoma receptor-1. Nature **391:**799–803.
3. **Ebisuno Y, Tanaka T, Kanemitsu N, Kanda H, Yamaguchi K, Kaisho T, Akira S, Miyasaka M.** 2003. Cutting edge: the B cell chemokine CXC chemokine ligand 13/B lymphocyte chemoattractant is expressed in the high endothelial venules of lymph nodes and Peyer's patches and affects B cell trafficking across high endothelial venules. J. Immunol. **171:**1642–1646.
4. **Carlsen HS, Baekkevold ES, Johansen FE, Haraldsen G, Brandtzaeg P.** 2002. B cell attracting chemokine 1 (CXCL13) and its receptor CXCR5 are expressed in normal and aberrant gut associated lymphoid tissue. Gut **51:**364–371.
5. **Yang D, Chen Q, Hoover DM, Staley P, Tucker KD, Lubkowski J, Oppenheim JJ.** 2003. Many chemokines including CCL20/MIP-3α display antimicrobial activity. J. Leukoc. Biol. **74:**448–455.
6. **Durr M, Peschel A.** 2002. Chemokines meet defensins: the merging concepts of chemoattractants and antimicrobial peptides in host defense. Infect. Immun. **70:**6515–6517.
7. **Chertov O, Yang D, Howard OMZ, Oppenheim JJ.** 2000. Leukocyte granule proteins mobilize innate host defenses and adaptive immune responses. Immunol. Rev. **177:**68–78.
8. **Wang W, Owen SM, Rudolph DL, Cole AM, Hong T, Waring AJ, Lal RB, Lehrer RI.** 2004. Activity of α- and θ-defensins against primary isolates of HIV-1. J. Immunol. **173:**515–520.
9. **Rodriguez-Garcia M, Climent N, Oliva H, Casanova V, Franco R, Leon A, Gatell JM, Garcia F, Gallart T.** 2010. Increased alpha-defensins 1–3 production by dendritic cells in HIV-infected individuals is associated with slower disease progression. PLoS One **5:**e9436. doi:10.1371/journal.pone.0009436.
10. **Reinhart TA, Fallert BA, Pfeifer ME, Sanghavi S, Capuano S, III, Rajakumar P, Murphey-Corb M, Day R, Fuller CL, Schaefer TM.** 2002. Increased expression of the inflammatory chemokine CXC chemokine ligand 9/monokine induced by interferon-gamma in lymphoid tissues of rhesus macaques during simian immunodeficiency virus infection and acquired immunodeficiency syndrome. Blood **99:**3119–3128.
11. **Murphey-Corb M, Martin LN, Rangan SRS, Baskin GB, Gormus BJ, Wolf RH, Andes WA, West M, Montelaro RC.** 1986. Isolation of an HTLV-III-related retrovirus from macaques with simian AIDS and its possible origin in asymptomatic mangabeys. Nature **321:**435–437.
12. **Choi YK, Fallert Junecko BA, Klamar CR, Reinhart TA.** 2013. Characterization of cells expressing lymphatic marker LYVE-1 in macaque large intestine during simian immunodeficiency virus infection identifies a large population of nonvascular LYVE-1(+)/DC-SIGN(+) cells. Lymphat. Res. Biol. **11:**26–34.
13. **Qin S, Fallert Junecko BA, Trichel AM, Tarwater PM, Murphey-Corb MA, Kirschner DE, Reinhart TA.** 2010. Simian immunodeficiency virus infection alters chemokine networks in lung tissues of cynomolgus macaques: association with Pneumocystis carinii infection. Am. J. Pathol. **177:**1274–1285.
14. **Qin S, Sui Y, Soloff AC, Fallert Junecko BA, Kirschner DE, Murphey-Corb MA, Watkins SC, Tarwater PM, Pease JE, Barratt-Boyes SM, Reinhart TA.** 2008. Chemokine and cytokine mediated loss of regulatory T cells in lymph nodes during pathogenic simian immunodeficiency virus infection. J. Immunol. **180:**5530–5536.
15. **Fallert BA, Reinhart TA.** 2002. Improved detection of simian immunodeficiency virus RNA by in situ hybridization in fixed tissue sections: combined effects of temperatures for tissue fixation and probe hybridization. J. Virol. Methods **99:**23–32.
16. **Basu S, Schaefer TM, Ghosh M, Fuller CL, Reinhart TA.** 2002. Molecular cloning and sequencing of 25 different rhesus macaque chemokine cDNAs reveals evolutionary conservation among C, CC, CXC, and CX3C families of chemokines. Cytokine **18:**140–148.
17. **Schaefer TM, Fuller CL, Basu S, Fallert BA, Poveda SL, Sanghavi SK,**

Choi Y-K, Kirschner DE, Feingold E, Reinhart TA. 2006. Increased expression of interferon-inducible genes in macaque lung tissues during simian immunodeficiency virus infection. Microbes Infect. **8:**1839–1850.
18. **Qin S, Sui Y, Murphey-Corb MA, Reinhart TA.** 2008. Association between decreased CXCL12 and CCL25 expression and increased apoptosis in lymphoid tissues of cynomolgus macaques during SIV infection. J. Med. Primatol. **37:**46–54.
19. **Zaragoza MM, Sankaran-Walters S, Canfield DR, Hung JK, Martinez E, Ouellette AJ, Dandekar S.** 2011. Persistence of gut mucosal innate immune defenses by enteric alpha-defensin expression in the simian immunodeficiency virus model of AIDS. J. Immunol. **186:**1589–1597.
20. **Ouellette AJ.** 2010. Paneth cells and innate mucosal immunity. Curr. Opin. Gastrenterol. **26:**547–553.
21. **Cash HL, Whitham CV, Behrendt CL, Hooper LV.** 2006. Symbiotic bacteria direct expression of an intestinal bactericidal lectin. Science **313:**1126–1130.
22. **Vaishnava S, Behrendt CL, Ismail AS, Eckmann L, Hooper LV.** 2008. Paneth cells directly sense gut commensals and maintain homeostasis at the intestinal host-microbial interface. Proc. Natl. Acad. Sci. U. S. A. **105:**20858–20863.
23. **Widney DP, Breen EC, Boscardin WJ, Kitchen SG, Alcantar JM, Smith JB, Zack JA, Detels R, Martinez-Maza O.** 2005. Serum levels of the homeostatic B cell chemokine, CXCL13, are elevated during HIV infection. J. Interferon Cytokine Res. **25:**702–706.
24. **Cagigi A, Mowafi F, Phuong Dang LV, Tenner-Racz K, Atlas A, Grutzmeier S, Racz P, Chiodi F, Nilsson A.** 2008. Altered expression of the receptor-ligand pair CXCR5/CXCL13 in B cells during chronic HIV-1 infection. Blood **112:**4401–4410.
25. **Chen L, Adams J, Steinman R.** 1978. Anatomy of germinal centers in mouse spleen, with special reference to "follicular dendritic cells." J. Cell Biol. **77:**148–164.
26. **Nossal GJV, Abbot A, Mitchell J, Lummus Z.** 1968. Antigens in immunity. J. Exp. Med. **127:**277–290.
27. **MacLennan ICM.** 1994. Germinal centers. Annu. Rev. Immunol. **12:**117–139.
28. **Lindqvist M, van Lunzen J, Soghoian DZ, Kuhl BD, Ranasinghe S, Kranias G, Flanders MD, Cutler S, Yudanin N, Muller MI, Davis I, Farber D, Hartjen P, Haag F, Alter G, Schulze zur Wiesch J, Streeck H.** 2012. Expansion of HIV-specific T follicular helper cells in chronic HIV infection. J. Clin. Invest. **122:**3271–3280.
29. **Petrovas C, Yamamoto T, Gerner MY, Boswell KL, Wloka K, Smith EC, Ambrozak DR, Sandler NG, Timmer KJ, Sun X, Pan L, Poholek A, Rao SS, Brenchley JM, Alam SM, Tomaras GD, Roederer M, Douek DC, Seder RA, Germain RN, Haddad EK, Koup RA.** 2012. CD4 T follicular helper cell dynamics during SIV infection. J. Clin. Invest. **122:**3281–3294.
30. **Vinuesa CG, Linterman MA, Goodnow CC, Randall KL.** 2010. T cells and follicular dendritic cells in germinal center B-cell formation and selection. Immunol. Rev. **237:**72–89.
31. **Lane HC, Masur H, Edgar LC, Whalen G, Rook AH, Fauci AS.** 1983. Abnormalities of B-cell activation and immunoregulation in patients with the acquired immunodeficiency syndrome. N. Engl. J. Med. **309:**453–458.
32. **Moir S, Malaspina A, Pickeral OK, Donoghue ET, Vasquez J, Miller NJ, Krishnan SR, Planta MA, Turney JF, Justement JS, Kottilil S, Dybul M, Mican JM, Kovacs C, Chun TW, Birse CE, Fauci AS.** 2004. Decreased survival of B cells of HIV-viremic patients mediated by altered expression of receptors of the TNF superfamily. J. Exp. Med. **200:**587–600.
33. **Moir S, Ho J, Malaspina A, Wang W, DiPoto AC, O'Shea MA, Roby G, Kottilil S, Arthos J, Proschan MA, Chun TW, Fauci AS.** 2008. Evidence for HIV-associated B cell exhaustion in a dysfunctional memory B cell compartment in HIV-infected viremic individuals. J. Exp. Med. **205:**1797–1805.
34. **Moir S, Fauci AS.** 2009. B cells in HIV infection and disease. Nat. Rev. Immunol. **9:**235–245.
35. **Salzman NH, Underwood MA, Bevins CL.** 2007. Paneth cells, defensins, and the commensal microbiota: a hypothesis on intimate interplay at the intestinal mucosa. Semin. Immunol. **19:**70–83.
36. **Ayabe T, Ashida T, Kohgo Y, Kono T.** 2004. The role of Paneth cells and their antimicrobial peptides in innate host defense. Trends Microbiol. **12:**394–398.
37. **Yang D, Chertov O, Bykovskaia SN, Chen Q, Buffo MJ, Shogan J, Anderson M, Schroder JM, Wang JM, Howard OM, Oppenheim JJ.** 1999. Beta-defensins: linking innate and adaptive immunity through dendritic and T cell CCR6. Science **286:**525–528.
38. **Singh SP, Zhang HH, Foley JF, Hedrick MN, Farber JM.** 2008. Human T cells that are able to produce IL-17 express the chemokine receptor CCR6. J. Immunol. **180:**214–221.
39. **Cole AM, Hong T, Boo LM, Nguyen T, Zhao C, Bristol G, Zack JA, Waring AJ, Yang OO, Lehrer RI.** 2002. Retrocyclin: a primate peptide that protects cells from infection by T- and M-tropic strains of HIV-1. Proc. Natl. Acad. Sci. U. S. A. **99:**1813–1818.
40. **Brenchley JM, Douek DC.** 2012. Microbial translocation across the GI tract. Annu. Rev. Immunol. **30:**149–173.
41. **Wong JM, de Souza R, Kendall CW, Emam A, Jenkins DJ.** 2006. Colonic health: fermentation and short chain fatty acids. J. Clin. Gastroenterol. **40:**235–243.
42. **Macfarlane GT, Macfarlane S.** 2011. Fermentation in the human large intestine: its physiologic consequences and the potential contribution of prebiotics. J. Clin. Gastroenterol. **45**(Suppl):S120–S127.
43. **Schauber J, Iffland K, Frisch S, Kudlich T, Schmausser B, Eck M, Menzel T, Gostner A, Luhrs H, Scheppach W.** 2004. Histone-deacetylase inhibitors induce the cathelicidin LL-37 in gastrointestinal cells. Mol. Immunol. **41:**847–854.
44. **Schauber J, Svanholm C, Termen S, Iffland K, Menzel T, Scheppach W, Melcher R, Agerberth B, Luhrs H, Gudmundsson GH.** 2003. Expression of the cathelicidin LL-37 is modulated by short chain fatty acids in colonocytes: relevance of signalling pathways. Gut **52:**735–741.
45. **Sanderson IR.** 2004. Short chain fatty acid regulation of signaling genes expressed by the intestinal epithelium. J. Nutr. **134:**2450S–2454S.
46. **Ochoa-Zarzosa A, Villarreal-Fernandez E, Cano-Camacho H, Lopez-Meza JE.** 2009. Sodium butyrate inhibits Staphylococcus aureus internalization in bovine mammary epithelial cells and induces the expression of antimicrobial peptide genes. Microb. Pathog. **47:**1–7.
47. **Fusunyan RD, Quinn JJ, Fujimoto M, MacDermott RP, Sanderson IR.** 1999. Butyrate switches the pattern of chemokine secretion by intestinal epithelial cells through histone acetylation. Mol. Med. **5:**631–640.